

Application of a ground-based, multi-channel microwave radiometer to the alerting of low-level windshear at an airport

P.W. CHAN* and Y.F. LEE

Hong Kong Observatory, Hong Kong, China

(Manuscript received December 25, 2010; in revised form May 1, 2011; accepted May 2, 2011)

Abstract

Low-level windshear, which refers to sustained changes of headwind of 15 knots (7.7 m/s) or more over a distance of several hundred metres to about 4 km, could be hazardous to the aircraft flying close to the ground. This paper presents the preliminary results in the application of a radiometer in the alerting of low-level windshear. A ground-based, 14-channel microwave radiometer (7 oxygen channels and 7 water vapour channels) has been in use at the Hong Kong International Airport since May 2008. The radiometer data were mostly collected in clear and cloudy weather conditions without significant rainfall. Two approaches to the alerting of windshear have been studied, namely, the calculation of Brunt-Vaisala frequency and the standard deviation of the brightness temperature measured by a microwave radiometer at the 60 GHz oxygen absorption complex. The former tries to represent the stability of the boundary layer of the atmosphere (terrain-induced windshear tends to occur in stable boundary layer) and the latter tries to correlate the wind fluctuations with the temperature fluctuations. The performance of the windshear alerting rules so developed is studied by the relative operating characteristics (ROC) curve balancing the hit rate of pilot windshear reports and the alert duration. It turns out that the Brunt-Vaisala frequency does not show much skill in the alerting. On the other hand, the brightness temperature fluctuations are found to have skills in capturing the windshear. By combining the alerts from brightness temperature fluctuations with the existing alerts issued by the Doppler Light Detection And Ranging (LIDAR) system, it may be possible to fully automate the issuance windshear alerts for a runway corridor of the Hong Kong International Airport (HKIA) without the need of subjective windshear warnings issued by the aviation weather forecasters, at least for terrain-induced windshear. The probability of detection (POD) for pilot windshear report reaches 89 % with the percentage of time on alert of 20 %. The POD is only less than that for the existing overall windshear alerting service (machined generated windshear alerts plus windshear warnings issued by the aviation weather forecasters) by about 4 %.

Zusammenfassung

Bodennahe Windscherungen, die dauerhafte Änderungen des horizontalen Windgeschwindigkeit von 7,7 m/s oder mehr hervorrufen, können gefährlich für bodennah fliegende Flugzeuge sein. Hier werden vorläufige Ergebnisse zur Erstellung von Windscherungswarnungen aus Radiometer-Daten vorgestellt. Seit April 2008 wird am internationalen Flughafen von Hong Kong ein 14-Kanal-Radiometer mit 7 Sauerstoff-Kanälen und sieben Wasserdampf-Kanälen betrieben. Die Daten wurden bei klarem und bei wolkeigem Wetter ohne signifikanten Niederschlag gewonnen. Zwei Herangehensweisen wurden untersucht, nämlich die Berechnung der Brunt-Vaisala-Frequenz und die Standard-Abweichung der Strahlungstemperatur im 60 GHz-Sauerstoff-Komplex. Die erste Methode versucht die Stabilität der Grenzschicht zu repräsentieren (thermisch induzierte Windscherung tritt in stabil geschichteten Grenzschichten auf), die zweite Methode versucht Wind-Fluktuationen mit Temperatur-Fluktuationen zu korrelieren. Die Effizienz der Warnungen wird mit der "Relative operating characteristics (ROC)"-Kurve untersucht, welche die Trefferrate mit Berichten der Piloten vergleicht. Es stellt sich heraus, dass die Brunt-Vaisala-Methode nicht sehr gut funktioniert, während die Strahlungstemperatur-Methode Potenzial hat. Durch Kombination von Warnungen mit der Strahlungstemperatur-Methode mit Alarmen, die auf Daten von Doppler-LIDAR-Geräten beruhen, könnte es möglich sein, ein voll automatisches Warnsystem für Windscherungen aufzubauen, ohne dass subjektive Warnungen von Flugmeteorologen benötigt werden. Dies gilt zumindest für gelände-induzierte Scherungen. Die Entdeckungswahrscheinlichkeit für solche Scherungen erreicht 89 %, wobei 20 % der Zeit mit Warnungen belegt sind. Diese Wahrscheinlichkeit ist nur 4 % niedriger als bei der gegenwärtigen Situation mit Warnungen, die auf maschinen-generierten Warnungen plus solchen von Beobachtern basieren.

1 Introduction

The Hong Kong International Airport (HKIA) is situated in an area of complex terrain. The geographical setup of Hong Kong is shown in Fig. 1. To the south of HKIA, there is the mountainous Lantau Island with

peaks rising to about 1000 m above mean sea level and valleys about 400 m in between. When wind climbs over the complicated terrain, airflow disturbances may occur downstream of the mountains, causing windshear and turbulence to the aircraft operating at HKIA. Windshear alerting service is operated by the Hong Kong Observatory (HKO), the meteorological authority in Hong Kong. One direct way of alerting windshear is to measure the winds along the flight paths. To this end, the Observatory

*Corresponding author: P.W. Chan, Hong Kong Observatory, 134A Nathan Road, Kowloon, Hong Kong, China, email: pwchan@hko.gov.hk

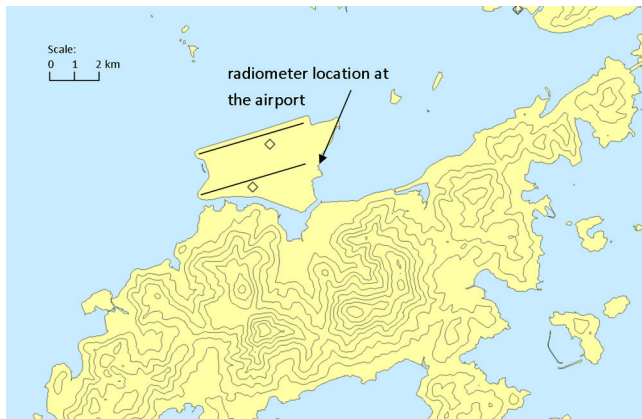


Figure 1: Locations of the meteorological instruments as mentioned in the text. The two spades indicate the locations of the LIDAR systems. The two straight lines are the north and the south runways respectively. Height contours are in 100 m.

has operated Doppler Light Detection And Ranging (LIDAR) systems to scan along the flight path and construct the headwind profiles to be encountered by the aircraft. The headwind data are analyzed automatically to examine the occurrence of significant changes of the wind, based on which windshear alerts are issued. LIDAR is used because it works well in clear air condition, and the majority of windshear at HKIA, as a result of terrain-disrupted airflow, occurs in non-rainy weather. In case of rain, conventional weather radars allow determining the wind speed due to scattering by rain droplets. A Terminal Doppler Weather Radar (TDWR) was also strategically located to monitor windshear and microbursts in the terminal area under rainy conditions.

This paper considers an alternative approach to the alerting of low-level windshear, namely, through the monitoring of stability of the boundary layer and fluctuations of the temperature. The temperature data are provided by a ground-based, remote-sensing instrument, namely, a multi-channel, passive microwave radiometer. They were collected in clear and cloudy weather conditions without significant rainfall; or if rain occurred, the rainfall rate was far less than 30 mm/hour, the rainfall rate threshold discussed in CHAN (2009) for reliable measurements to be available from the radiometer. For temperature fluctuations, only the brightness temperature of one single frequency channel is considered in this preliminary study. The radiometer-based windshear alerts, if found to show some skills, are also combined with the LIDAR-based windshear alerts in moving towards the full automation of windshear alerting. At present, apart from the LIDAR-based alerts and other sources of automatic windshear alerts, it is necessary for the aviation weather forecaster to monitor the weather condition and issue windshear warnings based on experience, so that the overall windshear alerting service (i.e. the machine-based automatic windshear alerts + the human-based windshear warnings) can capture at least 90 % of the windshear reports from pilots.

The applications of radiometer in the alerting of low-level windshear have been considered in studies in 1980s, by detecting gust fronts ahead of the aircraft (National Research Council, 1983). There have been recent research studies on the use of radiometer in the detection of mountain wave for aviation applications (WEST et al., 2009). The present paper considers the use of ground-based microwave radiometer in the alerting of windshear in an operational environment.

2 Instrument

A ground-based microwave radiometer (model: RPG HATPRO from Radiometer Physics) was permanently introduced to Hong Kong in February 2008. Some technical descriptions of this instrument could be found in ROSE et al. (2005). It consists of 14 channels, namely, 7 channels at the 60 GHz oxygen absorption complex (with frequencies 51.26, 52.28, 53.86, 54.94, 56.66, 57.30 and 58.00 GHz) and 7 channels along the 22.225 GHz water vapour absorption line (with frequencies 22.24, 23.04, 23.84, 25.44, 26.24, 27.84 and 31.40 GHz). Neural network retrieval method has been constructed to retrieve the temperature profiles from the brightness temperature measurements. In constructing the neural network, high-resolution (2 second) radiosonde data in the period 2003 to 2008 are used. In the present configuration, the radiometer mostly operates in the near-zenith mode, with a temporal resolution of one second. In the near-zenith mode, the elevation angle is 79.8 degrees with respect to the horizon instead of 90 degrees in order to avoid solar interference effect in the summer. This near-zenith mode gives all the quantities, namely, brightness temperatures as well as the quantities derived from brightness temperatures such as temperature profile, humidity profile, integrated water vapour (IWV), liquid water path (LWP) and cloud-base height. In about every 20 minutes, it also makes a boundary-layer scan, with elevation angles 90.0, 42.0, 30.0, 19.2, 10.2 and 5.4 degrees with respect to the horizon. The boundary-layer scan provides the temperature profile in the boundary layer only (up to a height of about 1.5 km above ground) and it increases the information on the temperature profile in the lowest 1 km (CREWELL and LÖHNERT, 2007).

According to the specifications of the radiometer, the channels in the oxygen band have a radiometric resolution of 0.2 K, and that for water vapour is 0.1 K. The radiometric resolution is defined as the standard deviation of the calibrated brightness temperature computed over a 30 minute period when the microwave radiometer views a stable cryogenic reference target using 1 second integration times. The retrieved temperature has an accuracy of 1 K between the ground and 1 km aloft, and 2 K above 1 km up to 10 km aloft (based on unpublished study report of the radiometer in a field campaign, by comparison with nearby tower measurements).

3 Application to low-level windshear

Windshear refers to a change in the wind direction and speed for more than a few seconds, resulting in a change in the headwind or tailwind encountered by an aircraft (HKO, IFALPA and GAPAN, 2010). The spatial scale of the wind change is from several hundred metres to about 4 km. The windshear is considered as significant when the headwind/tailwind change is 15 knots (7.7 m/s) or more. Windshear alerting service is in place at HKIA for detecting low-level windshear, i.e. windshear occurring below 1600 feet or within 3 nautical miles (5.6 km) away from the runway end. The alerts are mostly provided by wind-measuring equipment, either in situ instruments such as anemometers and weather buoys, or remote-sensing instruments such as Doppler LIDAR systems (SHUN and CHAN, 2008), TDWR and wind profilers. Some general remarks of windshear hazard are also given in PROCTOR et al. (2000).

For HKIA, the majority of windshear (about 70 % based on pilot windshear reports) is related to the complex terrain near the airport. In particular, for prevailing winds from the east through southeast to southwest, terrain-disrupted airflow may occur in the vicinity of HKIA as the winds climb over the mountainous terrain of Lantau Island to the south of the airport. Terrain-induced windshear is often associated with changes in the stability of the boundary layer of the atmosphere. For instance, as the air descends from the mountains of Lantau Island, the air may be warmed up due to Foehn effect (SHUN et al., 2003). If the air near the ground is potentially cooler, a temperature inversion occurs in the lowest part of the troposphere. Temperature profiles provided by the microwave radiometer can be a useful tool to assess the stability of the boundary layer and thus provide the signature of the occurrence of terrain-induced windshear. In fact, a windshear warning rule has been developed some years ago based on the Brunt-Vaisala frequency (N) determined from the virtual temperature data of a radio acoustic sounding system (RASS) near the northern coast of Lantau Island. When the RASS-determined N is larger than 0.025/s at a level within the boundary layer (O.S.M. Lee, private communication), windshear warning is to be issued for about half an hour. Otherwise, the windshear warning is to be withheld, even though the wind data provided by other instruments may suggest the occurrence of low-level windshear. Such a RASS-based warning rule is found to reduce the false alarm rate of windshear alerting service (O.S.M. Lee, private communication).

3.1 N -based windshear rule

In view of the previous results, the temperature data of the microwave radiometer are used to calculate N as a first attempt for their application in windshear alerting, using the following formula:

$$N = \sqrt{g \left| \frac{d \ln \theta}{dz} \right|}$$

where g is the acceleration due to gravity, z the height, and θ the potential temperature. Different thresholds for N are adopted, and windshear warning is issued for a period of T minutes when the radiometer-based N value exceeds the threshold within the past T minutes.

The performance of radiometer-based N rule is considered for spring-time (January to April) at HKIA, in which the terrain-induced windshear is the most common at the airport under the influence of cooler continental air originating from northern China. Radiometer data at spring-time have been collected for two years at the airport, namely, 2009 and 2010. The runway under consideration is 07RD (departing from the south runway to the east), with a total number of 160 pilot reports of significant windshear during the period. The radiometer-based N rule is examined using the relative operating characteristics (ROC) curve to strike a balance between percentage of detection (POD) of pilot windshear reports and the percentage of time on alert (POTA, or alert duration, expressed as the percentage of time when warnings/alerts are issued divided by the total time period under consideration). Only terrain-induced windshear is considered hereafter as we are looking at the stability of the boundary layer. The other two major types of low-level windshear, namely, sea breeze and thunderstorm, are not covered in this study. The ROC curve of radiometer-based N rule using the temperature data at all levels with the boundary-layer scan of the radiometer is given in Fig. 2, using a period $T = 60$ minutes. It could be seen that the radiometer-based N rule as such basically has no skill, namely, the ROC curve is close to the diagonal, and occasionally even lower than the diagonal. It turns out that, probably due to the characteristics of the training dataset for establishing the regression equations for temperature retrieval of the radiometer, there are persistently isothermal layers/temperature inversions in the lowest part and in the topmost part of the boundary-layer temperature profile. The one in the lowest part could be due to the discrepancy in temperature between the first reading of the radiosonde and the ground temperature measured at the upper-air ascent station. The one in the topmost part could be due to monsoon inversion that exists in south China coast. The existence of such features may result in too long alert duration, and thus reducing the skill level of the radiometer-based N rule. A sample set of boundary layer temperature data is tabulated in Fig. 2. As a result, in the next step the N values at the lowest and the topmost levels of the boundary-layer scan profile are not considered for capturing the pilot windshear reports. The resulting ROC curve with the removal of the lowest and the topmost levels of the boundary-layer scan of the radiometer is shown in Fig. 2 ($T = 60$ minutes only) and Fig. 3. It could be seen that the radiometer-based N rule becomes slightly more skillful, with the ROC curve lying above the diagonal. However, the skill level is not high as the ROC curve is still rather close to the diagonal. Similar skill levels are obtained with different validity periods of the N -based warning rules, namely, changing from a period T of 60 minutes to 10, 15 or 30

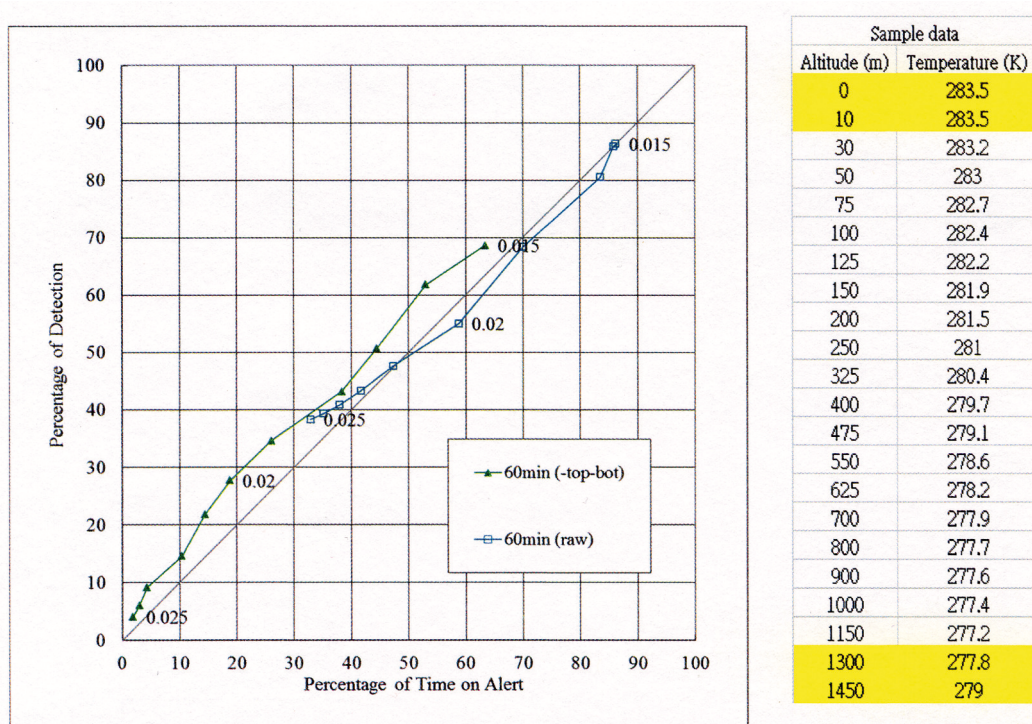


Figure 2: ROC curve for N -based windshear alerting rule based on the radiometer is shown on the left hand side. Both the use of the whole boundary layer temperature profiles (“raw”) and the removal of the topmost and the lowest parts of the profiles (“-top-bot”) are considered. The period under consideration includes the spring time of 2009 and 2010. A period $T = 60$ minutes is used. The right hand side shows a sample set of temperature retrieved from the boundary layer scan of the radiometer, with the “topmost part” and the “lowest part” highlighted in yellow. The thresholds are increased from 0.015 to 0.025 at steps of 0.001 (from right to left).

minutes (Fig. 3). In practical application, the radiometer-based N rule does not seem to be useful. The radiometer is expected to give more reliable temperature data than RASS in strong winds (mainly strong east to southeasterly winds in spring time) because the acoustic wavefronts are susceptible to distortion in high wind situation. The present results with the microwave radiometer indicate the limitations of the N -based windshear alerting rules. Based on the available results, it may be concluded that both RASS and radiometer have poor windshear warning skills by using the N -based rule, which may in general have rather strong limitations for the purpose of alerting low-level windshear. As such, other windshear alerting rules based on temperature data need to be explored.

3.2 Windshear rule based on standard deviation of brightness temperature

Apart from changing the stability of the atmosphere, the terrain-disrupted airflow may bring about rapid fluctuations of the brightness temperature measured by the microwave radiometer, which may be considered as an integral of the air temperature over a range of altitudes. For a ground-based radiometer pointing to zenith, well defined weighting function peaks for each frequency is observed (CREWELL et al., 2001). For 58 GHz, the normalized difference weighting function

reaches a maximum at an altitude of 400 to 500 m (manual of the radiometer, available at www.radiometer-physics.de/rpg/html/Download.html). As an example, the event of terrain-induced windshear leading to diversion of aircraft on 26–27 December 2009 as discussed in CHAN (2010) is examined. The time series of brightness temperature fluctuation as obtained in the near-zenith scan of the radiometer, namely, the standard deviation of brightness temperature at 58 GHz over each 10-minute time interval, is shown in Fig. 4, together with the timing of the pilot windshear reports over three runway corridors in use at HKIA, i.e. landing at the north runway from the west (07LA), landing at the south runway from the west (07RA) and departing south runway to the east (07RD). It appears from this example that the windshear reports were mostly received at times when standard deviation of 58-GHz brightness temperature was larger. Similar observations are obtained in other cases of terrain-induced windshear in the spring, and thus standard deviation of brightness temperature is tried out to develop another radiometer-based windshear warning rule. In the calculation of standard deviation, there is no consideration of removing the top and the bottom parts of the boundary layer temperature profile. However, because such a rule is developed, there is quality control issue with the brightness temperature to be overcome. As shown in a typical time series of 58-GHz brightness temperature in blue in Fig. 5, the tem-

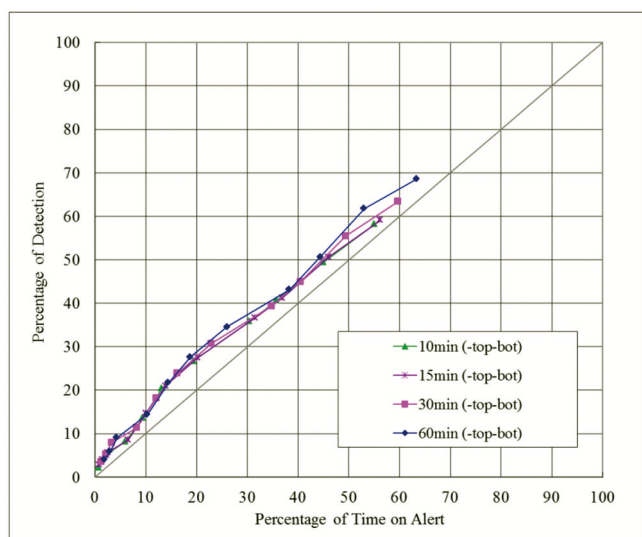


Figure 3: ROC curves for N -based windshear alerting rule based on the radiometer, for different periods T (10, 15, 30 and 60 minutes). The topmost and the lowest parts of the boundary layer temperature profile are removed. The data under consideration include the spring time of 2009 and 2010. The thresholds are increased from 0.015 to 0.025 at steps of 0.001 (from right to left).

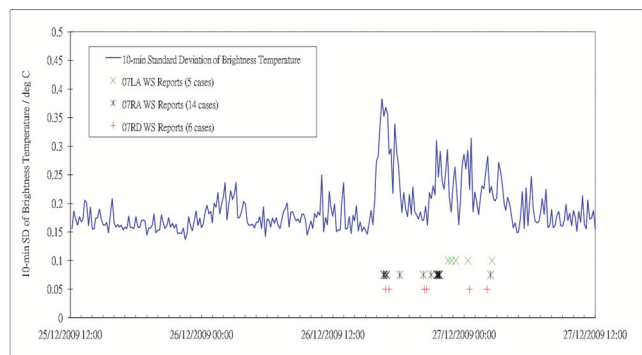


Figure 4: A sample time series of the standard deviation (SD) of 58-GHz brightness temperature measured by the radiometer in a case of terrain-induced windshear at HKIA. The windshear reports are given at the lower part of the figure, for the runway corridors 07LA (landing at the north runway from the west), 07RA (landing at the south runway from the west) and 07RD (departing from the south runway to the east).

perature values occasionally show some spikes reaching a few degrees K, which do not appear to be natural and may be related to noise probably arising from occasional interference from the environment (e.g. radars working at the airport). A quality-control procedure is then developed to remove such spikes, namely, at a particular time instance, the 58-GHz brightness temperature value is compared with the previous one (about a second ago) and the one before (about a couple of seconds ago). Two values of brightness temperature difference are then calculated. The brightness temperature at the point in time is considered acceptable only when both differences are less than or equal to 0.5 degrees K. The resulting quality-

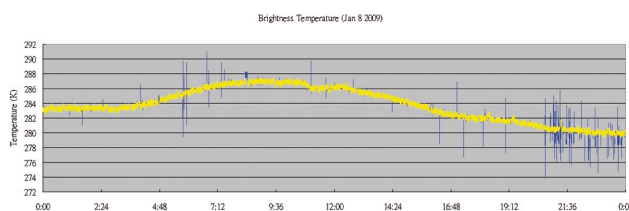


Figure 5: The raw (blue) and quality-controlled (yellow) 58-GHz brightness temperatures: a sample time series.

controlled brightness temperature time series is shown in yellow in Fig. 5. It could be seen that the majority of the spikes are effectively removed. The threshold of 0.5 degrees K is based on preliminary assessment only. More detailed analysis would be carried out to see how this threshold affects the capturing of low-level windshear.

With the quality-controlled brightness temperature time series, the performance of windshear warning rules based on brightness temperature fluctuations is studied. First of all, the whole time series of brightness temperature is divided into time intervals of 10 minute each. Within each time interval, the standard deviation of quality-controlled brightness temperature is calculated. At the end of each 10-minute interval, the previous M values of 10-minute standard deviations are considered. The first warning rule is based on the highest standard deviation in the past period of M times 10 minutes: when this highest standard deviation (among the M values) is larger than a prescribed threshold, windshear warning is automatically issued for a period of 10 minutes. Once again, only terrain-induced windshear is considered, and the period under study is the spring-time of 2009 and 2010. The runway corridor considered is 07RD, with 160 pilot reports of significant windshear. The resulting ROC curves based on different values of M ($= 1, 2, 3, 6$ and 9) are shown in Fig. 6. Compared to the ROC curve of the N -based rule in Fig. 3, it could be seen that the rule based on brightness temperature fluctuation is more skillful. The use of the longer period (i.e. the larger value of M) gives slightly better skill, though not significantly.

The windshear warning rule has also been revised slightly, namely, instead of considering the highest standard deviation value in the past period of M times 10 minutes, the second highest standard deviation value in this period (among the M values) is considered, namely, windshear warning for a period of 10 minutes is issued when the second highest standard deviation value is larger than a certain threshold. The resulting ROC curves are also shown in Fig. 6. It could be seen that the use of the second highest standard deviation is slightly more skillful than the use of the highest standard deviation value only in certain values of M , such as $M = 9$. As such, in the following discussion, the second highest standard deviation value in the past 90 minutes (i.e. $M = 9$) is considered for “brightness temperature fluctuation”, and once the threshold of 0.045 K is exceeded (threshold value indicated in Fig. 6), a windshear warn-

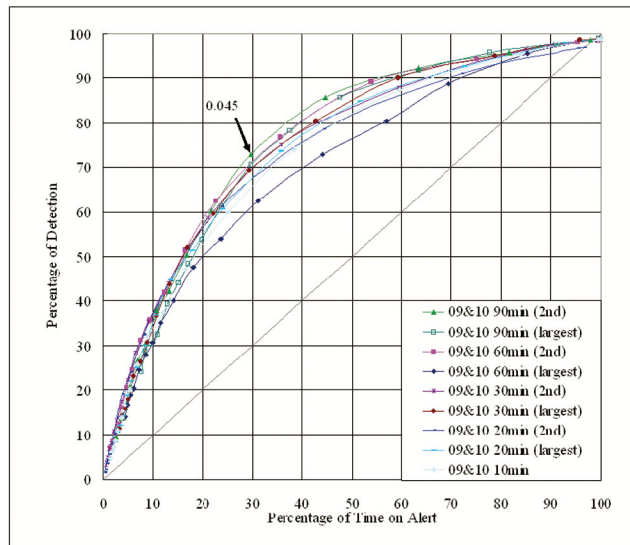


Figure 6: ROC curves for brightness temperature fluctuations: the largest standard deviation in the past period of M times 10 minutes (“largest”) and the second largest standard deviation in the same period (“2nd”). M is chosen to be 1, 2, 3, 6 and 9 (corresponding to past periods of 10, 20, 30, 60 and 90 minutes). The periods under consideration include the spring time of 2009 and 2010. The thresholds are increased from 0.005 to 0.1 at steps of 0.005 (from right to left).

ing is issued for 10 minutes. The threshold of 0.045 K is adopted because it is farthest away from the no skill line, with a probability of detection of 72 % and a percentage of time on alert of 30 %. The POTA of 30 % is still too large for the method to be practically useful in the alerting of low-level windshear for the aircraft, considering the POTA of the existing overall windshear alerting service (about 20 %).

The second highest standard deviation turns out to be slightly more skillful than the highest standard deviation. This may mean that we have to consider the temperature fluctuations that exceed a certain threshold for longer time, instead of simply having one standard deviation value (namely, the highest one) exceeding the threshold, in order to establish that the fluctuations persist for long enough time for the purpose of alerting the occurrence of terrain-disrupted airflow. This is particularly the case for the alerting of terrain-induced windshear, which is transient and sporadic in nature (HKO, IFALPA and GAPAN, 2010). In applying radiometer in the alerting of windshear, we would focus on those windshear situations that are more persistent. This is also the reason why a period of 90 minutes is considered in order to look for more persistent windshear features.

3.3 LIDAR + radiometer windshear alerts

Finally, a study is conducted to find out the skill level of automatically issuing windshear alerts only based on LIDAR and radiometer data as compared to the existing windshear alerting service, in which both machine-based windshear alerts from Windshear and Turbulence

Warning System (WTWS) and forecaster-issued windshear warnings are considered. The new windshear alerting rule is based on the union of LIDAR-based alerts (so called GLYGA, or G in short, see SHUN and CHAN (2008) for details) and radiometer-based alerts using brightness temperature fluctuation (or R in short). The resulting ROC curves for 07RD in spring time 2009 and 2010 are shown in Fig. 7. There are a couple of considerations:

(i) The skill level of “G or R” is clearly higher than “R only”, with the former ROC curve getting closer to the optimal performance location at the upper left corner of the diagram;

(ii) The skill level of “G or R” is rather close to the point of the existing windshear alerting service “WTWS + forecaster”. Given the same POTA (about 20 %), the POD of “G or R” is only slightly lower than that of “WTWS + forecaster” (89 % of the former vs. 93 % of the latter). A POTA of 20 % is considered reasonable in the provision of windshear alerting service for the aircraft, in view of the POTA value for the existing overall windshear alerting service.

Please note that the above results are obtained for spring time (January to April) of two years only (2009 and 2010). Data of more years are to be collected and studied. The study would also be expanded to cover other seasons, e.g. windshear in tropical cyclone situation and intense southwest monsoon in the summer, though the boundary layer of the atmosphere becomes neutral most of the time. Based on the available results, it appears that combination of LIDAR and radiometer alerts has the potential of replacing windshear warnings issued by the human weather forecasters altogether, in moving towards fully automatic issuance of alerts for the windshear alerting service. But it is necessary to note that the present results apply to terrain-induced windshear only. For HKIA, terrain-induced windshear is the major cause of low-level windshear, namely, it accounts for about 70 % of the pilot windshear reports. Thus the successful capturing of terrain-induced windshear would be very useful in the alerting of low-level windshear to be encountered by the aircraft. For information, sea breeze is the second major cause of windshear at HKIA, accounting for about 20 % of the pilot windshear reports. The remaining 10 % of the windshear reports arise from thunderstorms, gust fronts, microburst and low-level jets.

In Fig. 7, the data point labelled GLYGA corresponds to “G only”. There is not a ROC curve because, as discussed in SHUN and CHAN (2008), the GLYGA has adopted a fixed alerting threshold of 14 knots (7.2 m/s) only and there is no alerting threshold for fine-tuning. The combination of “WTWS + forecaster” also has a single data point only because, once again, there is no alerting threshold for tuning purpose. The curve “G or R” gives an indication about the additional value gained by combining the GLYGA alerts with the radiometer alerts, at least for terrain-induced windshear.

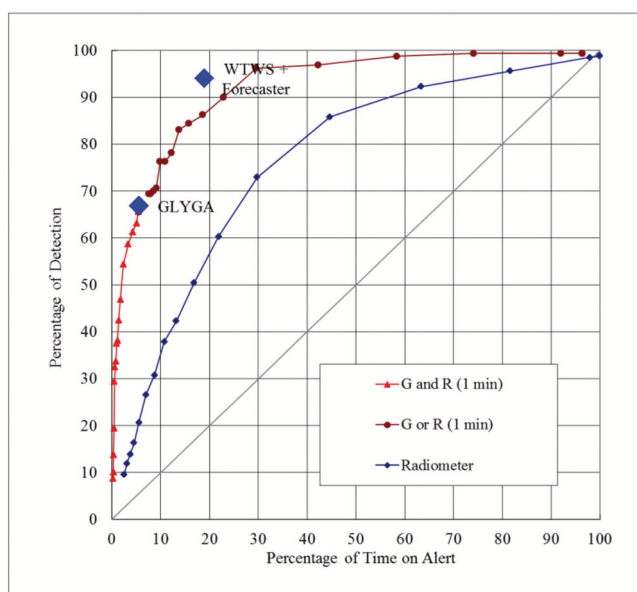


Figure 7: ROC curves for “G or R”, “G and R” (i.e. an alert is issued only when both GLYGA and radiometer issue windshear alerts at the same time), and the radiometer alone. For comparison, the performance values of GLYGA only and the overall windshear alerting service (WTWS + forecaster) are also given. There are single points only for the latter two because there are no alerting thresholds to fine-tune. The ROC curve for “G and R” only gets to the point of GLYGA only because this is the point where no radiometer alerts are used. On the other hand, the ROC curve for “G or R” starts from the point of GLYGA because this is the point from which radiometer alerts start to be considered. The thresholds are increased from 0.005 to 0.1 at steps of 0.005 (from right to left).

4 Conclusions

The application of microwave radiometer in the alerting of low-level windshear is studied in the present paper. The radiometer data were collected in clear and cloudy weather conditions without significant rainfall. Firstly, it is shown that the radiometer-based threshold on the Brunt-Vaisala frequency N does not appear to have skills in capturing windshear. On the other hand, based on standard deviation of the 58-GHz brightness temperature, there are skills in capturing the pilot windshear reports as shown in the ROC curve deviating significantly from the diagonal. In this process, quality control of the raw brightness temperature data from the radiometer is required, and the use of the second highest standard deviation value in the last 90 minutes shows better skills than the use of the highest standard deviation value only.

The use of LIDAR alone has a probability of detection of 67 % and a percentage of time on alert of 5 %. It is also possible to combine the LIDAR-based and the radiometer-based windshear rules for fully automatic windshear alerting. The skill level of the resulting alerts is very close to that of the overall windshear alerting service at present, namely, machine-based windshear alerts

plus windshear warnings issued by the human weather forecasters. With the same POTA at 20 %, the POD of pilot windshear reports only differs by about 4 % (89 % for LIDAR + radiometer, vs. 93 % of the existing windshear alerting service). This shows the potential of implementing completely automatic windshear alerts by combining the alerts generated by different meteorological instruments, at least for terrain-induced windshear. Please note that the present results are obtained for terrain-induced windshear at HKIA for a runway corridor and based on 160 pilot reports only. A larger dataset would be used in future studies to better establish the feasibility of using radiometer in the alerting of low-level windshear.

References

- CHAN, P.W., 2009: Performance and application of a multi-wavelength, ground-based microwave radiometer in intense convective weather. – *Meteorol. Z.* **18**, 253–265.
- , submitted: A significant windshear event leading to aircraft diversion at the Hong Kong International Airport. – *Meteor. Appl.*
- CREWELL, S., H. CZEKALA, U. LÖHNERT, C. SIMMER, TH. ROSE, R. ZIMMERMANN, R. ZIMMERMANN, 2001: Microwave Radiometer for Cloud Cartography: A 22-channel ground-based microwave radiometer for atmospheric research. – *Radio Sci.* **36**, 621–638.
- CREWELL, S., U. LÖHNERT, 2007: Accuracy of boundary layer temperature profiles retrieved with multi-frequency, multi-angle microwave radiometry. – *IEEE Transactions Geosci. Rem. Sens.* **45**, 2195–2201.
- HKO, IFALPA AND GAPAN, 2010: Windshear and Turbulence in Hong Kong. – Information booklet for pilots, 3rd Edition.
- NATIONAL RESEARCH COUNCIL, 1983: Low-altitude wind shear and its hazard to aviation. National Academy Press. – available at <http://books.google.com.hk/books?id=RUNuGXuyZhkC&printsec=frontcover#v=onepage&q&f=false>.
- PROCTOR, F.H., D.A. HINTON, R.L. BOWLES, 2000: A windshear hazard index. – 9th Conference on Aviation, Range, and Aerospace Meteorology, Orlando, FL, American Meteorological Society.
- ROSE, T., S. CREWELL, U. LOHNERT, C. SIMMER, 2005: A network suitable microwave radiometer for operational monitoring of the cloudy atmosphere. – *Atmos. Res.* **75**, 183–200.
- SHUN, C.M., P.W. CHAN, 2008: Applications of an infrared Doppler Lidar in detection of wind shear. – *J. Atmos. Ocean. Technol.* **25**, 637–655.
- SHUN, C.M., C.M. CHENG, O.S.M. LEE, 2003: LIDAR observations of terrain-induced flow and its application in airport wind shear monitoring. – International Conference on Alpine Meteorology (ICAM) and Mesoscale Alpine Programme (MAP) Meeting, Brig, Switzerland, 19–23 May 2003.
- WEST, L.L., and co-authors, 2009: Hazard detection analysis for a forward-looking interferometer. – 1st AIAA Atmospheric and Space Environments Conference, 22–25 June 2009, San Antonio, Texas, USA.